



FREE FIELD MEASUREMENTS OF THE EFFECTIVE ACOUSTIC PROPERTIES OF RIGIDLY BACKED ANISOTROPIC POROUS MATERIALS

Mélanie Nolan^{1,2*}

Lino Morin¹

Samuel A. Verburg²

Kirill Horoshenkov³

Jean-Philippe Groby¹

¹ Laboratoire d'Acoustique de l'Université du Mans, LAUM - UMR CNRS 6613
Le Mans Université, Avenue Olivier Messiaen, 72085 Le Mans Cedex 9, France

² Acoustic Technology, Department of Electrical and Photonics Engineering
Technical University of Denmark, Building 352, Ørsteds Plads, DK-2800 Kgs. Lyngby, Denmark

³ Department of Mechanical Engineering, University of Sheffield
Sheffield, S1 3JD, United Kingdom

ABSTRACT

Porous media can be described as effective anisotropic fluid materials that are characterized by a bulk modulus and a full symmetric density tensor. This paper presents a method for retrieving the bulk modulus and all six components of the density tensor from reflection coefficients measured in free field with an array of microphones. The procedure consists in expressing the sound field measured in the vicinity of a rigidly backed porous layer as a superposition of plane waves, from which the surface impedance and the reflection coefficient are reconstructed at the layer's surface. The reflection properties, as well as the pressure at the rigid backing interface, are estimated for various source positions (corresponding to various angles of incidence) and an inverse problem is formulated to infer the effective fluid parameters. The validity of the method is examined numerically on a synthetic porous material, and experimentally on a manufactured porous material.

Keywords: *Anisotropic porous media, angle-dependent surface impedance, microphone arrays*

*Corresponding author: melnola@dtu.dk.

Copyright: ©2023 Nolan et al. This is an open-access article distributed under the terms of the Creative Commons Attribution 3.0 Unported License, which permits unrestricted use, distribution, and reproduction in any medium, provided the original author and source are credited.

1. INTRODUCTION

Acoustic wave propagation and viscothermal dissipation of acoustic energy in porous media can be described macroscopically by an equivalent fluid model [1,2], which requires the knowledge of several pore parameters. Although some of the pore parameters can be measured directly, these methods require specialized equipment and are often difficult to carry out [3, 4]. Indirect acoustic methods, whereby a measurable acoustical property can be directly related to the pore morphology, are an attractive alternative to direct measurements. In particular, the normal incidence reflection and transmission coefficients are directly measurable with a standardized impedance tube and can be used to predict the behaviour of the dynamic density and bulk modulus of the equivalent fluid [5,6]. If the material is homogeneous and isotropic, these two frequency-dependent fluid parameters are also sufficient to determine the pore parameters that control the dissipation of acoustic energy in the medium [7]. Yet, it has been demonstrated that porous materials are not isotropic (i.e., their properties are a function of orientation) [8, 9], and that the influence of anisotropy translates in an equivalent density tensor (in place of a scalar).

In a recent numerical study, Terroir et al. [10] proposed a method for retrieving the bulk modulus and all six components of the density tensor of a layer of homogeneous anisotropic fluid material surrounded on both sides

by a homogeneous isotropic fluid. The procedure evaluates the reflection and transmission coefficients at various angles of incidence, from which an inverse problem is formulated to infer the effective material parameters. This paper extends on the methodology proposed in Terroir et al. by considering a rigidly-backed anisotropic porous layer, and examines if the bulk modulus and density tensor can be inferred experimentally, from reflection coefficients measured in free field with an array of microphones. The procedure is based on a recent experimental method developed in [11, 12], which consists in estimating the surface impedance at oblique incidence via sound field reconstruction (sound pressure and particle velocity) at the material's surface.

2. THEORY

Let us consider a layer of homogeneous anisotropic fluid material Ω with thickness L , bulk modulus B and density tensor ρ . In the reference coordinate system $(O, \mathbf{e}_1, \mathbf{e}_2, \mathbf{e}_3)$ with position coordinates (x_1, x_2, x_3) , its boundaries are defined by the equations $x_3 = 0$ and $x_3 = L$. The layer is fixed on a rigid impervious wall at $x_3 \leq 0$ and surrounded by a homogeneous isotropic fluid Ω_0 with bulk modulus B_0 and scalar density ρ_0 on the other side ($x_3 \geq L$). We further assume that the density tensor ρ is symmetric; that is ${}^t\rho = \rho$, where t denotes transposition. In particular, the orthonormal coordinate system $(\mathbf{e}_I, \mathbf{e}_{II}, \mathbf{e}_{III})$ of the layer's principal directions can be defined so that the density tensor is diagonal in this system; that is $\rho = \rho^* = \text{diag}(\rho_I, \rho_{II}, \rho_{III})$, where ρ_I, ρ_{II} and ρ_{III} are the principal densities. In the reference coordinate system, the density tensor reads $\rho = \mathbf{R} \cdot \rho^* \cdot {}^t\mathbf{R}$, where $\mathbf{R} = \mathbf{R}_3(\theta_{III})\mathbf{R}_2(\theta_{II})\mathbf{R}_1(\theta_I)$ is the rotation matrix between the two coordinate systems, with $\mathbf{R}_1, \mathbf{R}_2$ and \mathbf{R}_3 being elementary matrices of rotations and θ_I, θ_{II} and θ_{III} the roll, pitch and yaw angles, respectively.

2.1 Direct problem

The pressure and velocity fields in the layer are governed by the equations of mass and momentum conservation

$$j\omega \frac{p}{B} = \nabla \cdot \mathbf{v}, \quad j\omega \rho \cdot \mathbf{v} = \nabla p, \quad (1)$$

where ω is the angular frequency and time dependency $e^{-j\omega t}$ is omitted.

We now consider the incident plane wave $p^i = e^{j(k_1 x_1 + k_2 x_2 - k_3(x_3 - L))}$ propagating in the domain $x_3 \geq L$ with unit amplitude and the wavenumbers $k_1 =$

$-k_0 \sin(\theta) \cos(\phi)$, $k_2 = -k_0 \sin(\theta) \sin(\phi)$ and $k_3 = k_0 \cos(\theta)$, where k_0 is the wavenumber in Ω_0 and θ and ϕ are the elevation and azimuth angles measured from (O, x_3) and (O, x_1) , respectively. The Snell-Descartes law yields the specularly reflected wave $p^r = R e^{j k_3(x_3 - L)} e^{j \mathbf{k}_\Gamma \cdot \mathbf{x}_\Gamma}$, where R is the pressure reflection coefficient, $\mathbf{k}_\Gamma = k_1 \mathbf{e}_1 + k_2 \mathbf{e}_2$, and $\mathbf{x}_\Gamma = x_1 \mathbf{e}_1 + x_2 \mathbf{e}_2$. In the layer, the pressure and particle velocity fields take the form

$$p = \hat{p}(x_3) e^{j \mathbf{k}_\Gamma \cdot \mathbf{x}_\Gamma}, \quad (2a)$$

$$\mathbf{v} = \hat{\mathbf{v}}(x_3) e^{j \mathbf{k}_\Gamma \cdot \mathbf{x}_\Gamma}, \quad (2b)$$

where $\hat{p}(x_3)$ and $\hat{\mathbf{v}}(x_3)$ are independent of \mathbf{x}_Γ due to the layer being homogeneous. Substituting Eqs (2a) and (2b) into Eq. (1) yields the equations of apparent mass and momentum conservation

$$j\omega \frac{\hat{p}}{B} = j(\mathbf{q} \cdot \mathbf{k}_\Gamma) \hat{v}_3 + \frac{\partial \hat{v}_3}{\partial x_3}, \quad (3a)$$

$$j\omega \tilde{\rho} \hat{v}_3 = j(\mathbf{q} \cdot \mathbf{k}_\Gamma) \hat{p} + \frac{\partial \hat{p}}{\partial x_3}, \quad (3b)$$

where $\hat{v}_3 = \hat{\mathbf{v}}(x_3) \cdot \mathbf{e}_3$, $\mathbf{q} = q_1 \mathbf{e}_1 + q_2 \mathbf{e}_2$ is a dimensionless vector, and B and $\tilde{\rho}$ are the apparent bulk modulus and density, respectively. As in [10], the system of differential Eqs (3a) and (3b) can be written in a matrix form and solved by means of a matrix exponential provided the boundary conditions

$$\hat{p}(0) = p_0, \quad \hat{v}_3(0) = 0, \quad (4a)$$

$$\hat{p}(L) = 1 + R, \quad \hat{v}_3(L) = (R - 1)/\tilde{Z}_0, \quad (4b)$$

where p_0 is the sound pressure at the rigid backing, and $\tilde{Z}_0 = (\tilde{\rho}_0 B_0)^{1/2} = Z_0 / \cos(\theta)$ is the apparent impedance of air in the direction defined by \mathbf{e}_3 . This leads to the following expressions for the reflection coefficient R and the sound pressure at the rigid backing p_0

$$R = \frac{\cos(\tilde{k}L) + \frac{\tilde{Z}_0}{Z} j \sin(\tilde{k}L)}{\cos(\tilde{k}L) - \frac{\tilde{Z}_0}{Z} j \sin(\tilde{k}L)}, \quad (5a)$$

$$p_0 = \frac{2e^{j(\mathbf{q} \cdot \mathbf{k}_\Gamma)L}}{\cos(\tilde{k}L) - \frac{\tilde{Z}_0}{Z} j \sin(\tilde{k}L)}, \quad (5b)$$

with

$$\tilde{k} = \omega \sqrt{\tilde{\rho}/B}, \quad \tilde{Z} = \sqrt{\tilde{\rho}B} \quad (6)$$

the apparent wavenumber and impedance, respectively.

2.2 Inverse problem

The inverse problem consists in retrieving the values of the bulk modulus B and the six components of the symmetric density tensor $\rho_{11}, \rho_{12}, \rho_{13}, \rho_{22}, \rho_{23}$ and ρ_{33} (or, more conveniently, the six components of the inverse density tensor $\mathbf{H} = \boldsymbol{\rho}^{-1}$: $H_{11}, H_{12}, H_{13}, H_{22}, H_{23}$ and H_{33}) from reflection coefficients measured at specific angles of incidence; that is, for specific values of $\mathbf{k}_\Gamma = (k_1, k_2)$. Once estimated, the material parameters will be marked ($B^\dagger, H_{11}^\dagger, H_{12}^\dagger, H_{13}^\dagger, H_{22}^\dagger, H_{23}^\dagger, H_{33}^\dagger$). The system in Eqs (5a) and (5b) can be inverted as follows [10]

$$\tilde{Z} = \pm \tilde{Z}_0 \sqrt{\frac{(R+1)^2 - \frac{(p_0 e^{-j(\mathbf{q} \cdot \mathbf{k}_\Gamma)L})^2}{(R-1)^2}}{(R-1)^2}}, \quad (7a)$$

$$e^{\pm j\tilde{k}L} = \left[R \left(1 \pm \frac{\tilde{Z}}{\tilde{Z}_0} \right) + \left(1 \mp \frac{\tilde{Z}}{\tilde{Z}_0} \right) \right] \frac{1}{p_0 e^{-j(\mathbf{q} \cdot \mathbf{k}_\Gamma)L}}, \quad (7b)$$

which shows that the apparent impedance and wavenumber (and subsequently the apparent density and bulk modulus) can be directly retrieved from the reflection coefficient and sound pressure at the rigid backing, assuming prior knowledge of the phase delay $(\mathbf{q} \cdot \mathbf{k}_\Gamma)L$. The coefficients q_1 and q_2 of the vector \mathbf{q} and the apparent density $\tilde{\rho}$ can be shown to depend only on the inverse density tensor according to [10]

$$q_1 = \frac{H_{13}}{H_{33}}, \quad q_2 = \frac{H_{23}}{H_{33}}, \quad \tilde{\rho} = \frac{1}{H_{33}}. \quad (8)$$

Similarly, the apparent bulk modulus \tilde{B} can be shown to depend on the inverse density tensor, the physical bulk modulus B and the wavenumber vector \mathbf{k}_Γ according to [10]

$$\frac{\omega^2}{B} - \frac{\omega^2}{\tilde{B}(k_1, k_2)} = \xi_{11}k_1^2 + \xi_{22}k_2^2 + 2\xi_{12}k_1k_2, \quad (9)$$

with $\xi_{ij} = H_{ij} - H_{33}q_iq_j, \forall (i, j) \in \{1, 2\}^2$.

The coefficients q_1 and q_2 can be retrieved using two pairs of incident waves $\mathbf{k}_\Gamma = \pm k'_1 \mathbf{e}_1$ and $\mathbf{k}_\Gamma = \pm k'_2 \mathbf{e}_2$

$$e^{2jq_1k'_1L} = \frac{p_0(k'_1, 0)}{p_0(-k'_1, 0)}, \quad e^{2jq_2k'_2L} = \frac{p_0(0, k'_2)}{p_0(0, -k'_2)}, \quad (10)$$

and, at normal incidence, the physical bulk modulus can be retrieved from Eq. (9) as follows

$$B = \tilde{B}(0, 0). \quad (11)$$

Besides, the coefficients ξ_{11}, ξ_{22} and ξ_{12} can be inferred from Eq. (9) using $(k'_1, 0), (0, k'_2)$ and a sixth incident wave (k''_1, k''_2) as follows

$$\xi_{11} = \frac{\omega^2}{k_1'^2} \left(\frac{1}{B} - \frac{1}{\tilde{B}(k'_1, 0)} \right), \quad (12a)$$

$$\xi_{22} = \frac{\omega^2}{k_2'^2} \left(\frac{1}{B} - \frac{1}{\tilde{B}(0, k'_2)} \right), \quad (12b)$$

$$\xi_{12} = \frac{\omega^2}{2k_1''k_2''} \left(\frac{1}{B} - \frac{1}{\tilde{B}(k''_1, k''_2)} \right) - \frac{\xi_{11}k_1''}{2k_2''} - \frac{\xi_{22}k_2''}{k_1''}. \quad (12c)$$

Finally, the coefficients H_{13}, H_{23} and H_{33} are retrieved from Eq. 8, and the coefficients H_{12}, H_{11} and H_{22} from $H_{12} = \xi_{12} - H_{33}q_1q_2, H_{11} = \xi_{11} - H_{33}q_1^2$ and $H_{22} = \xi_{22} - H_{33}q_2^2$, respectively.

2.3 Estimation of the reflection coefficient at oblique incidence

The method is described in Refs [11] and [12]. The procedure relies on estimating the material surface impedance with an array of microphones, from which the reflection coefficient is calculated. The surface impedance is estimated via sound field reconstruction at the material surface (sound pressure and particle velocity), using a plane-wave expansion of the measured sound field.

Concisely, for the incident plane wave p^i propagating with unit amplitude and the wavenumbers k_1, k_2 and k_3 , the reflected field is the plane wave p^r propagating with a symmetrical direction of propagation with respect to the material surface and an amplitude characterized by a plane wave reflection coefficient R defined as

$$R = \frac{Z_S \cos(\theta) - 1}{Z_S \cos(\theta) + 1}, \quad (13)$$

where Z_S is the material normalized surface impedance. We now consider a microphone array placed in close proximity to the material surface. The measured pressures at the M microphone positions can be represented locally as a superposition of N propagating plane waves, with directions of propagation uniformly distributed over a spherical domain [13]. The problem can be expressed with the underdetermined linear model

$$\mathbf{p} = \mathbf{W}\mathbf{a}, \quad (14)$$

where $\mathbf{p} \in \mathbb{C}^M$ contains the measured pressures, $\mathbf{a} \in \mathbb{C}^N$ contains the unknown plane-wave amplitudes, and $\mathbf{W} \in \mathbb{C}^{M \times N}$ is a sensing matrix containing the plane-wave functions $W_{mn} = e^{j\mathbf{k}_n \cdot \mathbf{r}_m}$. Equation (14) can be solved using Tikhonov regularization [13]

$$\hat{\mathbf{a}} = \arg \min_{\mathbf{a}} (\|\mathbf{W}\mathbf{a} - \mathbf{p}\|_2^2 + \lambda \|\mathbf{a}\|_2^2), \quad (15)$$

where λ is a regularization parameter selected automatically using the L-curve criterion [14]. Once the vector $\hat{\mathbf{a}}$ has been estimated, the pressure \hat{p} and normal component of the particle velocity \hat{v}_n can be reconstructed at any point \mathbf{r}_S of the material's surface, as a sum of plane waves. A point-wise normalized surface impedance is calculated

$$Z_S(\mathbf{r}_S) = -\frac{1}{\rho_0 c_0} \frac{\hat{p}(\mathbf{r}_S)}{\hat{v}_n(\mathbf{r}_S)}, \quad (16)$$

which is then averaged over a small surface to smooth out random errors due to noise. Finally, the reflection coefficient is calculated from the plane wave model in Eq. (13).

3. NUMERICAL RESULTS

The validity of the retrieval method is examined numerically by means of simulated measurements in Matlab. As in Ref. [10], we consider a synthetic periodic porous layer of thickness $L = 3$ cm, formed by the repetition of an ellipsoidal unit cell. This anisotropic porous layer is described in the orthonormal coordinate system $(\mathbf{e}_I, \mathbf{e}_{II}, \mathbf{e}_{III})$ of the layer principal directions with a diagonal density tensor. Each principal density ρ_J with $J = I, II, III$ of the diagonal density tensor, as well as the bulk modulus B are approximated using the Johnson-Champoux-Allard-Lafarge (JCAL) model for rigid-framed porous media [2] (in this case, the JCAL model relies on homogenized properties of the unit cell, that are calculated using the multiple-scale method [15]). The parameters of the JCAL model are listed in Table 1. Note that some of these parameters are scalar quantities (porosity ϕ , thermal characteristic length Λ' and static thermal permeability $k'_{0,J}$), while others are tensorial quantities (high-frequency limit of the tortuosity $\alpha_{\infty,J}$, viscous characteristic length Λ_J and static viscous permeability $k_{0,J}$). The diagonal matrix density $\boldsymbol{\rho}^*$ is further rotated by the roll, pitch and yaw angles $\theta_I = \pi/6$, $\theta_{II} = \pi/4$ and $\theta_{III} = \pi/3$ to result in the fully-anisotropic density tensor (or, equivalently, its inverse). The air properties are calculated from the temperature $T = 20^\circ\text{C}$ and the atmospheric pressure $P_0 = 101320$ Pa [16].

The array used for the simulated measurement consists of 162 microphones, arranged in two square layers of 81 microphones each, with a vertical spacing of 3 cm between the two layers and a horizontal spacing of 2.5 cm. The array aperture is 20 cm x 20 cm. The array is placed at a distance of 1.5 cm from the material surface. 256 plane waves are used for the plane wave expansion, which directions of propagation are uniformly distributed over a spherical domain. 400 point-wise impedances are estimated at the material's surface on a grid of dimensions 10 cm x 10 cm. Gaussian noise is added to the simulated pressure with a SNR of 40 dB. The sound pressure p_0 at the rigid backing is simulated using Eq. (5b), to which Gaussian noise is added with the same SNR of 40 dB. The following incidence angles (ϕ, θ) are used for retrieving the bulk modulus and the six components of the inverse density tensor: $(0, \pi/3)$, $(\pi, \pi/3)$, $(\pi/2, \pi/6)$, $(-\pi/2, \pi/6)$, $(0, 0)$, $(\pi/3, \pi/4)$. The results are displayed for the center frequencies of the 1/3 octave bands spanning from 500 Hz to 4 kHz.

Table 1. Values of the JCAL parameters (from [10]).

ϕ	0.91
k'_0 [m ²]	8×10^{-9}
$k_{0,I}$ [m ²]	4.4×10^{-9}
$k_{0,II}$ [m ²]	3.2×10^{-9}
$k_{0,III}$ [m ²]	3.6×10^{-9}
Λ' [m]	3.68×10^{-4}
Λ_I [m]	2.04×10^{-4}
Λ_{II} [m]	2.4×10^{-4}
Λ_{III} [m]	2.68×10^{-4}
$\alpha_{\infty,I}$	1.18
$\alpha_{\infty,II}$	1.06
$\alpha_{\infty,III}$	1.04

Figure 1 shows the reconstructed reflection coefficient for the six angles of incidence considered in the retrieval procedure. This reflection coefficient, obtained from the reconstructed surface impedance and Eq. (13), is in excellent agreement with that of the direct problem [obtained from Eq. (5a)]. Once the reflection coefficient has been estimated, the retrieval method is applied to retrieve the bulk modulus and the six components of the inverse density tensor (see Figs 2 and 3). The retrieved parameters are

in good agreement with those used in the direct problem.

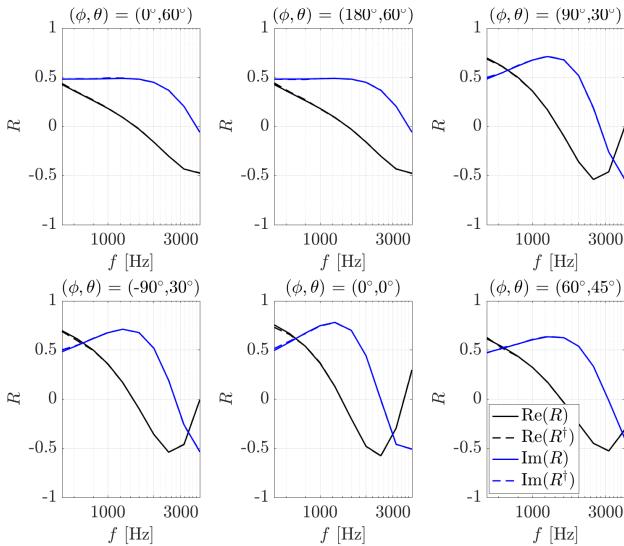


Figure 1. Reconstructed and initial real and imaginary parts of the reflection coefficient for the six angles of incidence considered in the retrieval procedure.

4. EXPERIMENTAL RESULTS

The validity of the proposed method is tested experimentally in a large (1000 m³) anechoic chamber at the Technical University of Denmark. The setup consists of a 2.4 m x 2.4 m layer of glass wool (thickness 10 cm, Saint-Gobain Ecophon, Hyllinge, Sweden) placed on a backing plate, an omnidirectional source, a programmable robotic arm equipped with a microphone and programmed to recreate the same array as in the simulated measurements in Sec. 3, and an additional microphone flush-mounted at the interface between the porous layer and the backing plate. The experimental results are not available at the time of this writing.

5. CONCLUSION

An experimental procedure has been proposed for retrieving the bulk modulus and all six components of the density tensor of a rigidly-backed layer of homogeneous anisotropic porous material. The procedure relies on measuring the reflection coefficient in free field at various

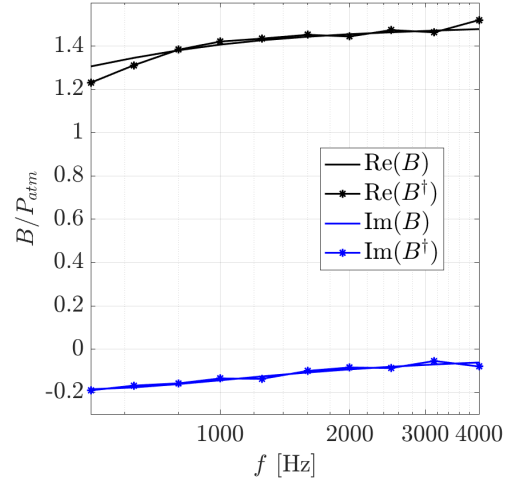


Figure 2. Reconstructed and initial real and imaginary parts of the normalized bulk modulus.

angles of incidence with an array of microphones. Future work includes a comparison of the resulting parameters with experimental results obtained from reflection and transmission coefficients measured in an impedance tube.

6. ACKNOWLEDGMENTS

The authors would like to thank Antoine Richard for discussions on the reconstruction of reflection coefficients, Henrik Hvidberg for help with the experimental arrangement, and Saint-Gobain Ecophon for providing the samples. This work is funded by the Independent Research Fund Denmark, under DFF-International Postdoctoral Grant 1031-00012.

7. REFERENCES

- [1] D. L. Johnson, J. Koplik, and R. Dashen, “Theory of dynamic permeability and tortuosity in fluid saturated porous media,” *J. Fluid Mech.*, vol. 176, pp. 379–402, 1987.
- [2] D. Lafarge, P. Lemarinier, J.-F. Allard, and V. Tarnow, “Dynamic compressibility of air in porous structures at audible frequencies,” *J. Acoust. Soc. Am.*, vol. 102, pp. 1995–2006, 1997.
- [3] K. V. Horoshenkov, A. Khan, F.-X. Bécot, L. Jaouen, F. Sgard, A. Renault, N. Amirouche, F. Pompoli,

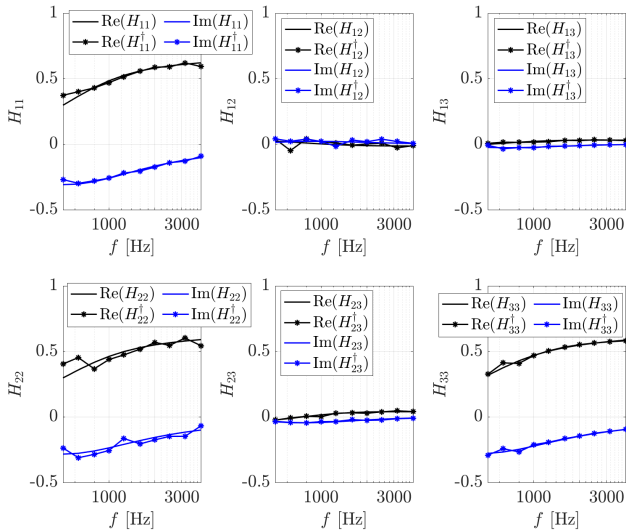
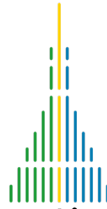


Figure 3. Reconstructed and initial real and imaginary parts of the six components of the symmetric inverse density tensor.

N. Prodi, P. Bonfiglio, G. Pispola, F. Asdrubali, J. Hubelt, N. Atalla, C. K. Amédin, W. Lauriks, and L. Boeckx, “Reproducibility experiments on measuring acoustical properties of rigidframe porous media (round-robin tests),” *J. Acoust. Soc. Am.*, vol. 122, pp. 345–353, 2007.

- [4] F. Pompoli, P. Bonfiglio, K. V. Horoshenkov, A. Khan, L. Jaouen, F.-X. Bécot, F. Sgard, F. Asdrubali, F. D’Alessandro, J. Hubelt, N. Atalla, C. K. Amédin, W. Lauriks, and L. Boeckx, “How reproducible is the acoustical characterization of porous media?,” *J. Acoust. Soc. Am.*, vol. 141, pp. 945–955, 2017.
- [5] K. Attenborough, “Acoustical characteristics of porous materials,” *Phys. Rep.*, vol. 82, pp. 179–227, 1982.
- [6] B. H. Song and J. S. Bolton, “A transfer-matrix approach for estimating the characteristic impedance and wave numbers of limp and rigid porous materials,” *J. Acoust. Soc. Am.*, vol. 107, pp. 1131–1152, 2000.
- [7] K. Attenborough, “The prediction of oblique-incidence behaviour of fibrous absorbents,” *J. Sound Vib.*, vol. 14, pp. 183–191, 1971.

- [8] W. J. Price and H. B. Huntington, “Acoustic properties of anisotropic materials,” *J. Acoust. Soc. Am.*, vol. 22, no. 1, pp. 32–37, 1950.
- [9] J.-F. Allard, R. Bourdier, and A. L’Esperance, “Anisotropy effects in glass wool on normal impedance in oblique incidence,” *J. Sound Vib.*, vol. 114, no. 2, pp. 233–238, 1987.
- [10] A. Terroir, L. Schwan, T. Cavalieri, V. Romero-Garcia, G. Gabard, and J.-P. Groby, “General method to retrieve all effective acoustic properties of fully anisotropic fluid materials in three-dimensional space,” *J. Appl. Phys.*, vol. 125, p. 025114, 2019.
- [11] A. Richard, E. Fernandez-Grande, J. Brunskog, and C.-H. Jeong, “Estimation of surface impedance at oblique incidence based on sparse array processing,” *J. Acoust. Soc. Am.*, vol. 141, no. 6, pp. 4115–4125, 2017.
- [12] A. Richard and E. Fernandez-Grande, “Comparison of two microphone array geometries for surface impedance estimation (I),” *J. Acoust. Soc. Am.*, vol. 146, no. 1, pp. 501–504, 2019.
- [13] M. Nolan, S. A. Verburg, J. Brunskog, and E. Fernandez-Grande, “Experimental characterization of the sound field in a reverberation room,” *J. Acoust. Soc. Am.*, vol. 145, no. 4, pp. 2237–2246, 2019.
- [14] P. C. Hansen, “Analysis of discrete ill-posed problems by means of the l-curve,” *SIAM Rev.*, vol. 34, pp. 561–580, 1992.
- [15] C. Auriault, J.-L. Boutin, and C. Geindreau, *Homogenization of coupled phenomena in heterogeneous media*. London: ISTE Ltd and Wiley, 2009.
- [16] A. D. Pierce, *Acoustics: An Introduction to Its Physical Principles and Applications*. New York: Acoustical Society of America, 1989.